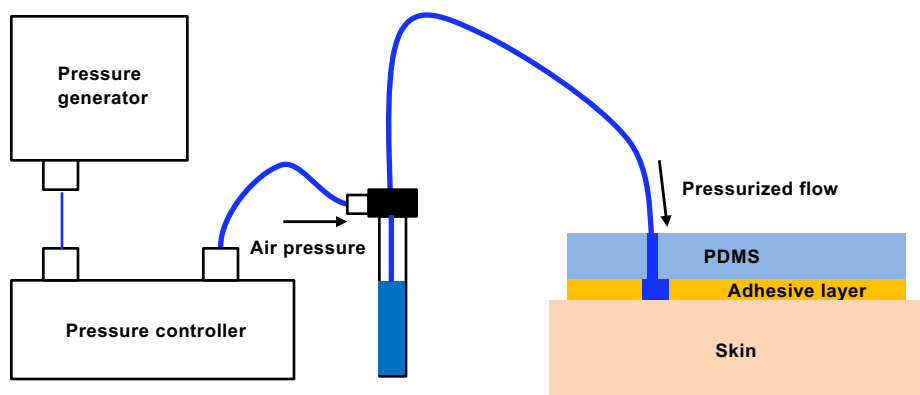
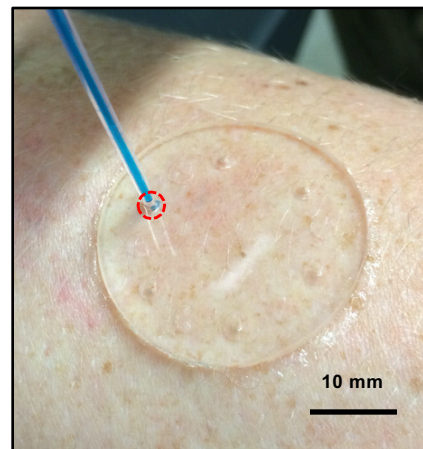


Fig. S1 a) Pressure leakage tests by use of a hydrostatic pressure generator. The device includes a PDMS layer with a 1 mm diameter hole connected to the opening (3 mm in diameter) in the adhesive layer. Tubing connected to the pressure source supplies blue dyed water at a desired pressure to a hole through the PDMS layer while on the skin. The blue dyed water fills the opening region of the adhesive. b) The tubing connects to the PDMS device with opening to the skin. c) Images of test results from different applied pressures 5, 10 and 15 kPa. d) Example of leakage of liquid between the adhesive and the skin. Red dotted circles define the adhesive opening in b-d. Scale bars represent 10 mm in b and c, 3 mm in d.

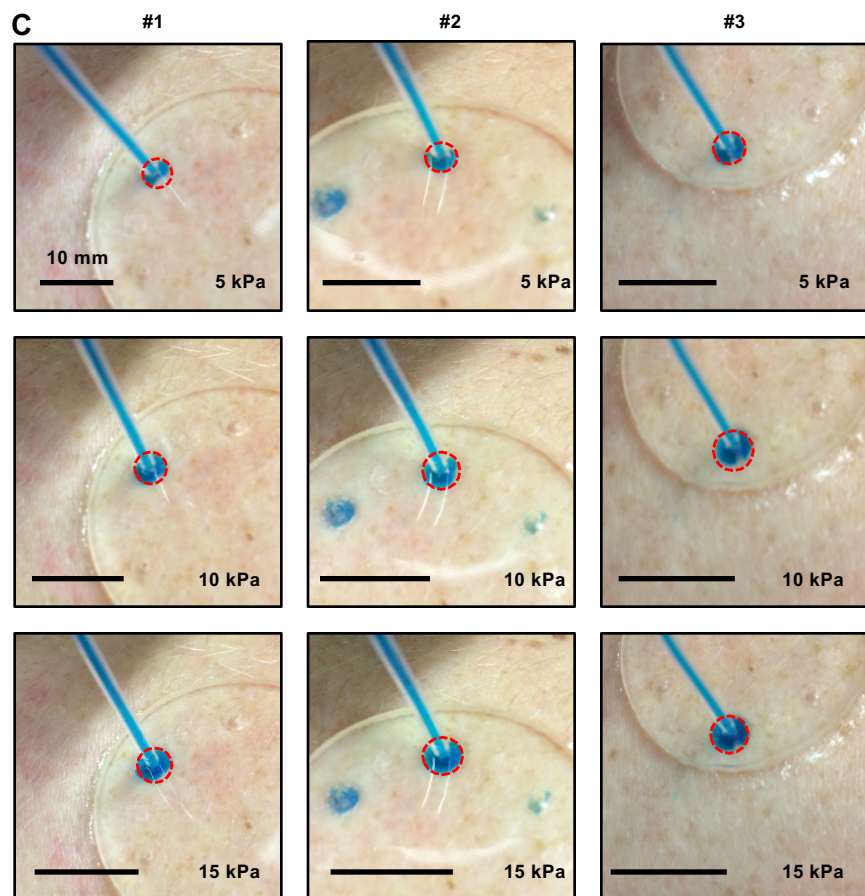
A



B



C



D

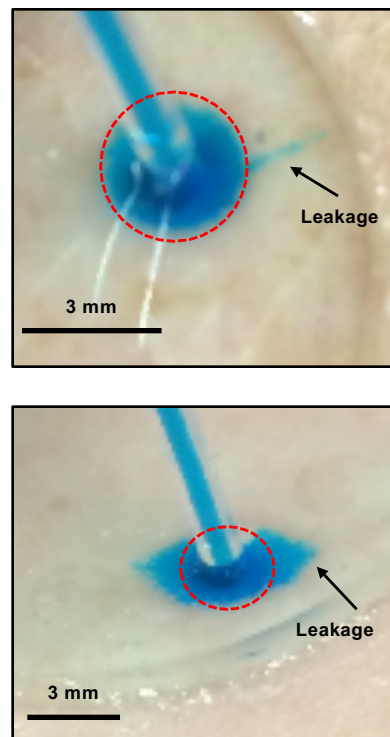


Fig. S2 The procedure of fabrication of the device.

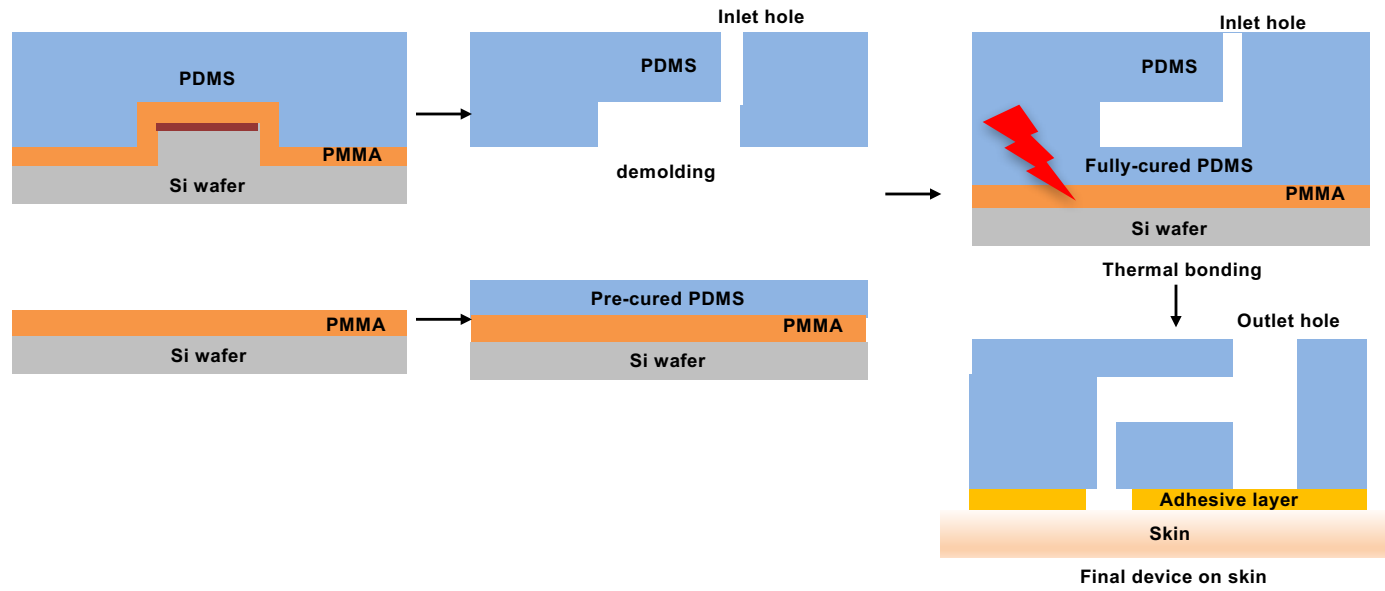
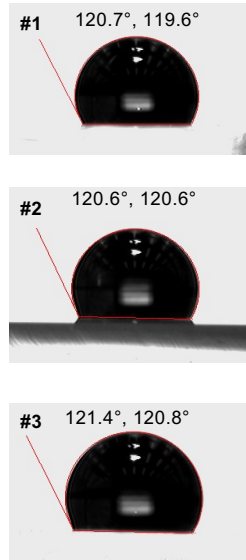
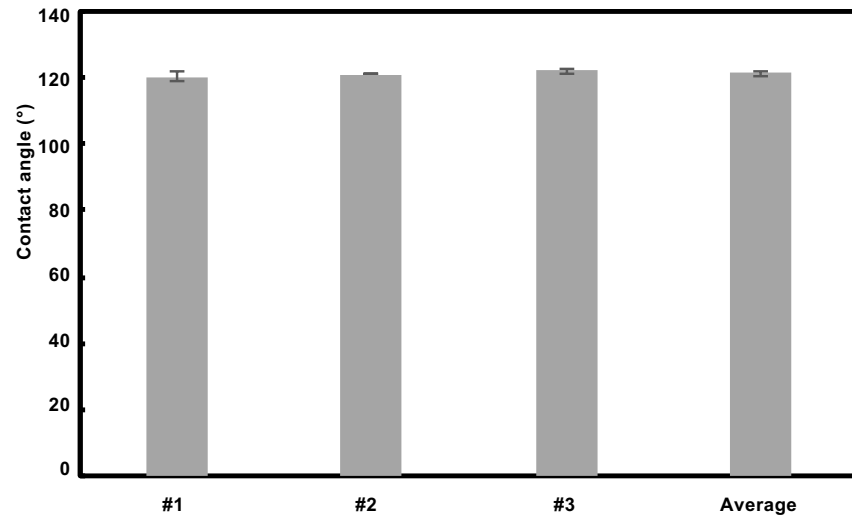


Fig. S3 Static and advancing contact angle of water to PDMS surface obtained from pre-cured PDMS

A



B



C

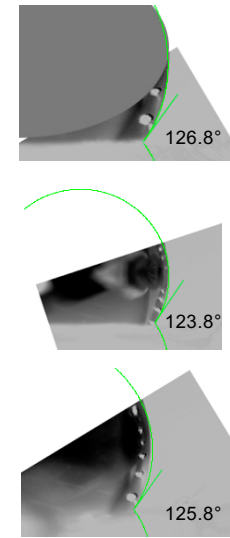


Fig. S4 a) the schematic of epidermal device to measure the secretory pressure in sweat glands. b) measured bursting pressure of the CBVs c) in situ test of the single CBV device d) the results of the in situ test of measurement of the secretory pressure of sweat glands

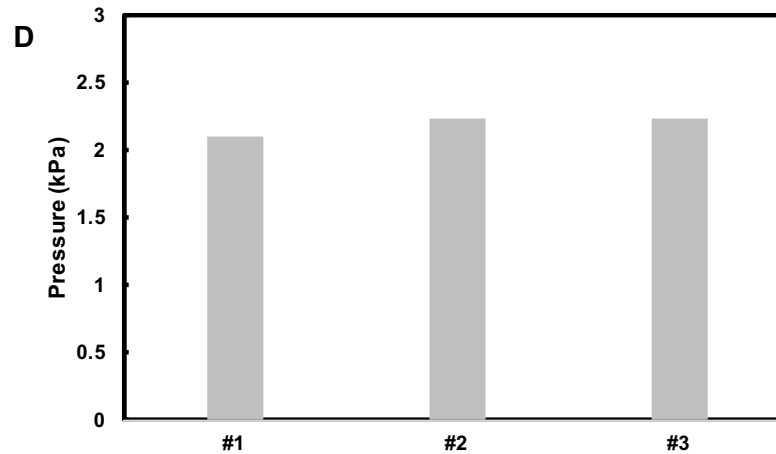
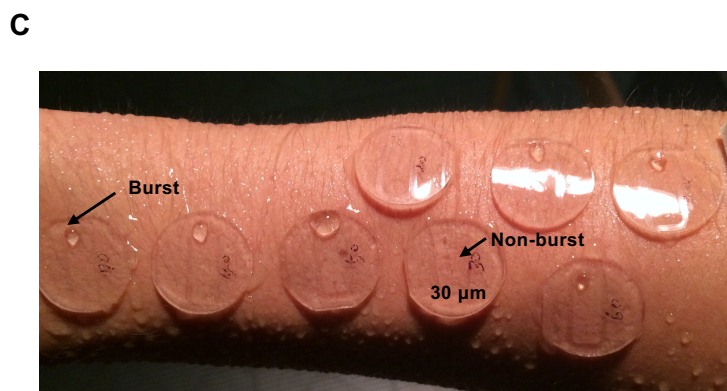
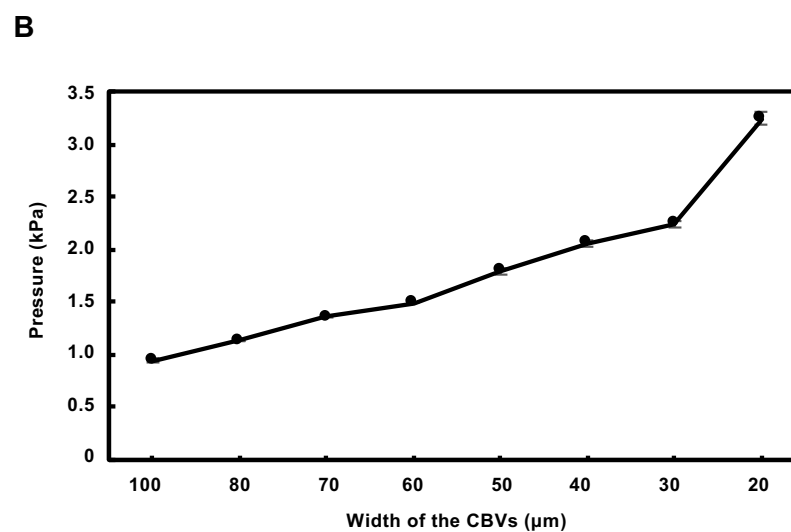
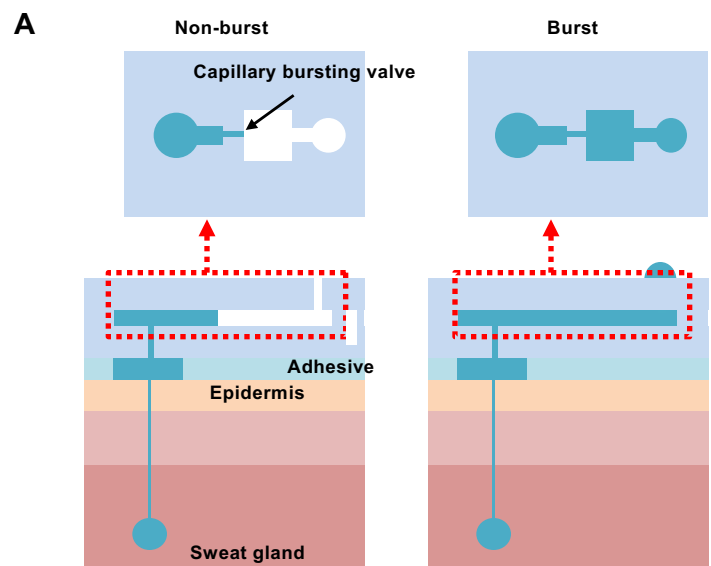


Fig. S5 a) the process of introducing CoCl_2 in 2% pHEMA into the chamber. b) the change of color of indicator applying of $0.3 \mu\text{L}$ of water. c) Volume of the channel that leads to the CBV and the main chamber.

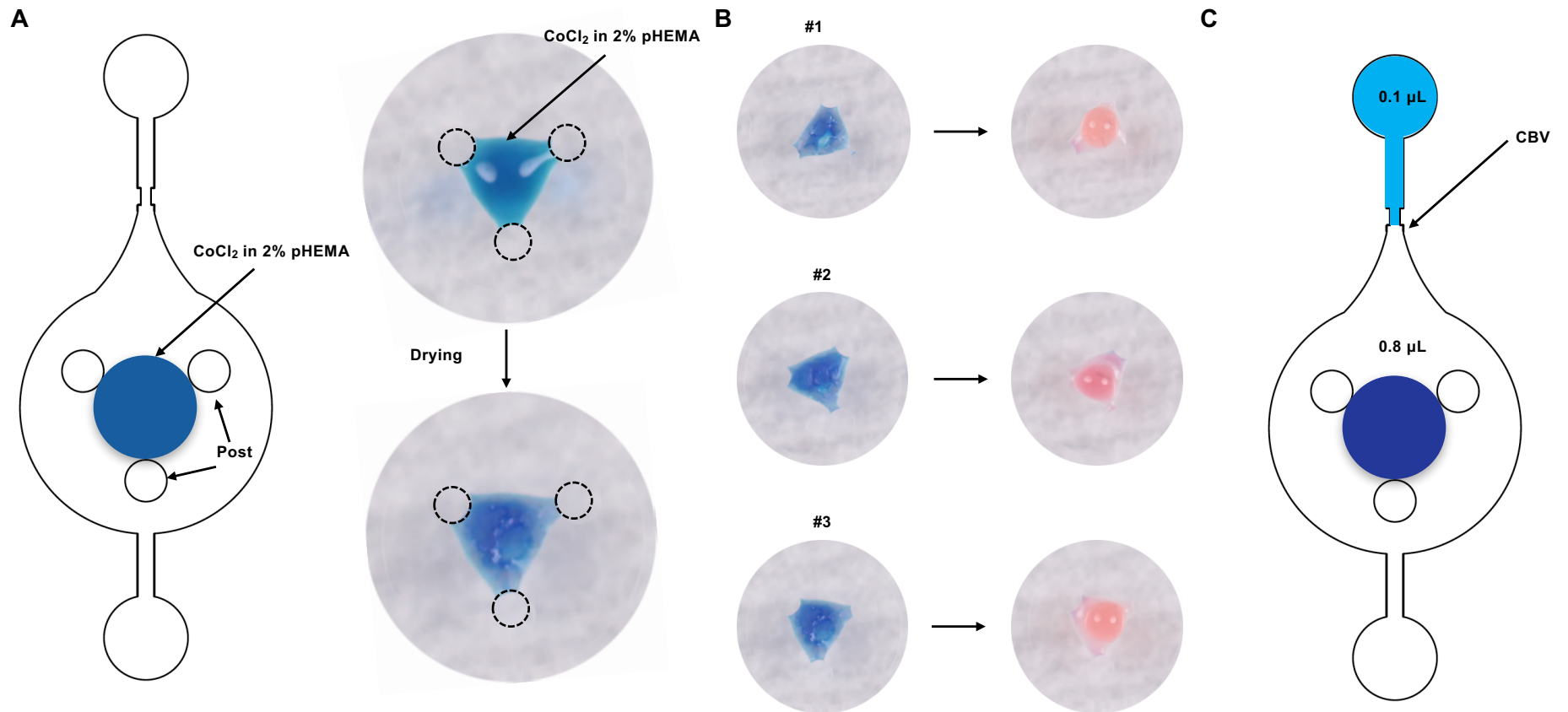


Fig. S6 a) Illustration of microfluidic channels with capillary bursting valve and rounding edge. b) Bursting pressure (component BP_b) of CBVs with different widths predicted by numerical simulation and theoretical calculation. Two-dimensional (2D) model is adopted in numerical simulation by assuming the CBV has infinite thickness, which neglects the BP_h in equation (2).

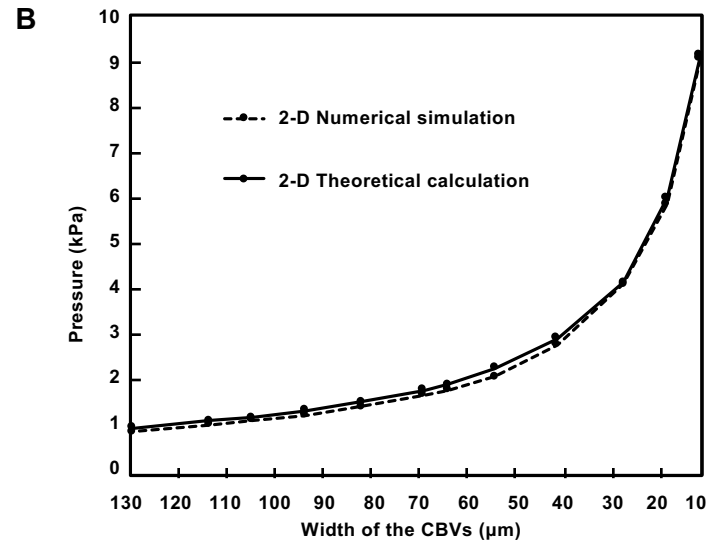
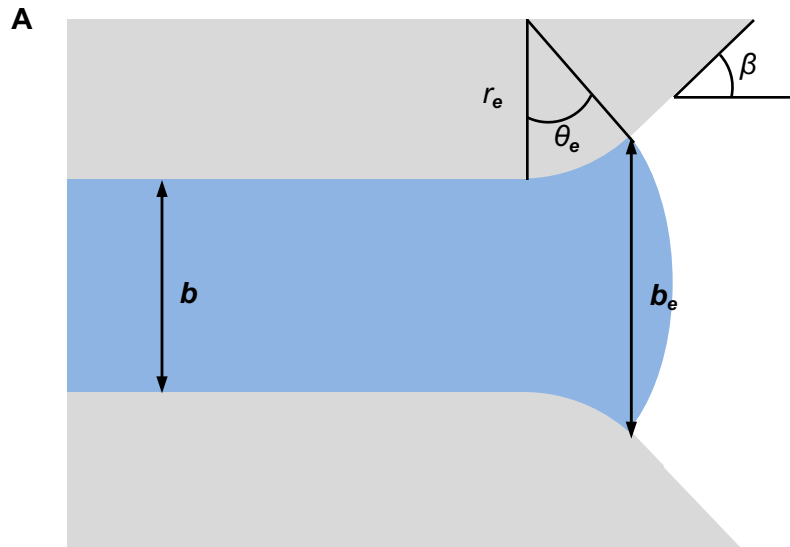


Fig. S7 In vitro pressure measurement set up

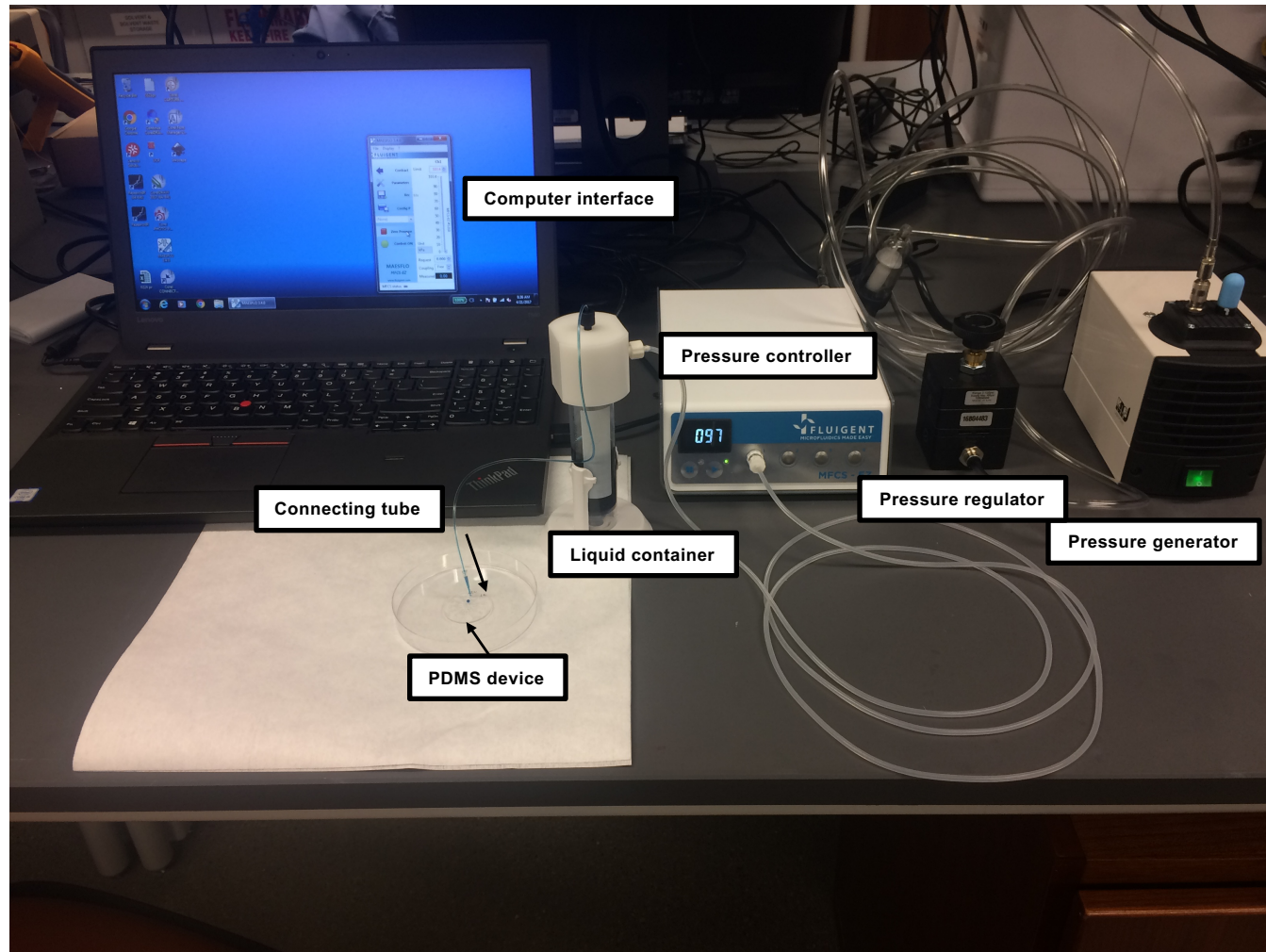


Fig. S8 a) Top view illustration of microfluidic channels with 12 same CBVs. b) Optical images of measurement of pressure of sweat gland from cycling exercise from different devices of different CBVs of 120, 110 and 100 μm . Red circle represents non-burst CBVs and green circle represents burst CBV.

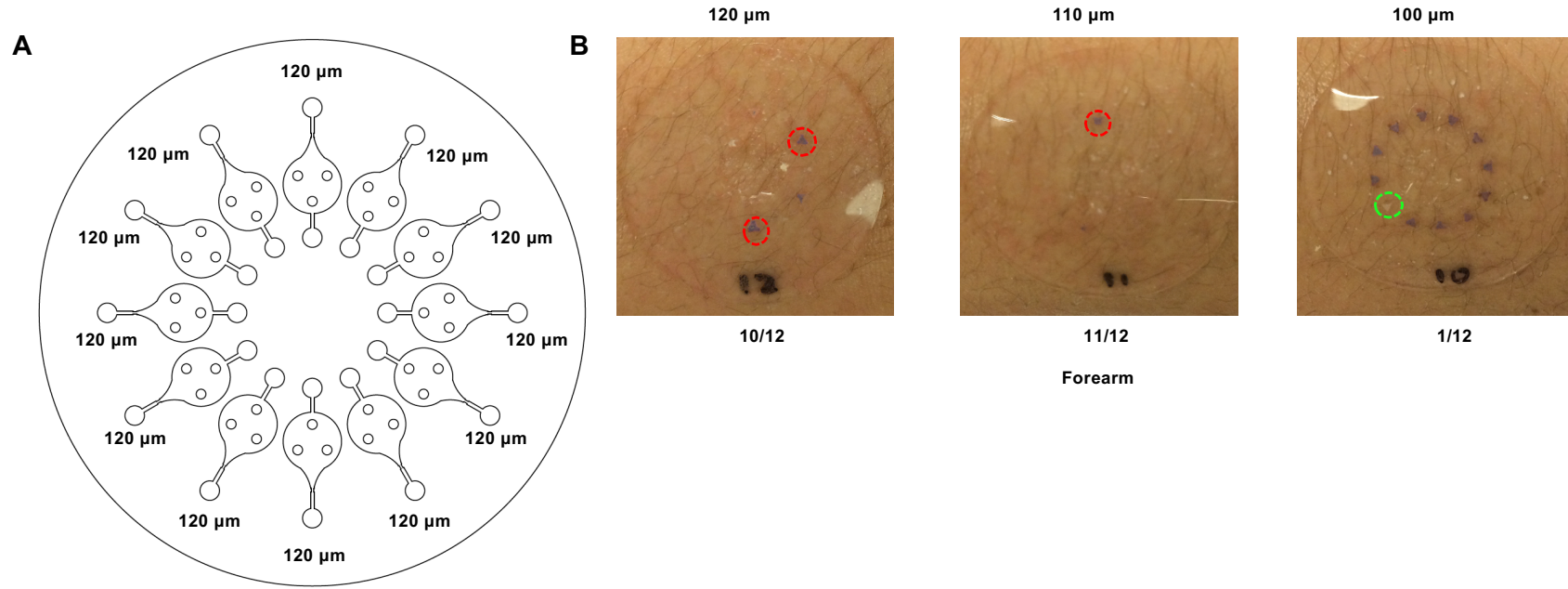


Fig. S9 a) Top view illustration of microfluidic channels with serial CBVs according to the width of the channel. Inset shows optical image of a device with CoCl_2 in 2% pHEMA at the center of each chamber b) SEM images of the CBVs at #1, #6 and #9. c) Optical image of a device filled by blue-dyed water at different bursting pressure. d) The bursting pressure of the CBVs from experimental test and theoretical calculation with rounding effect and without rounding effect.

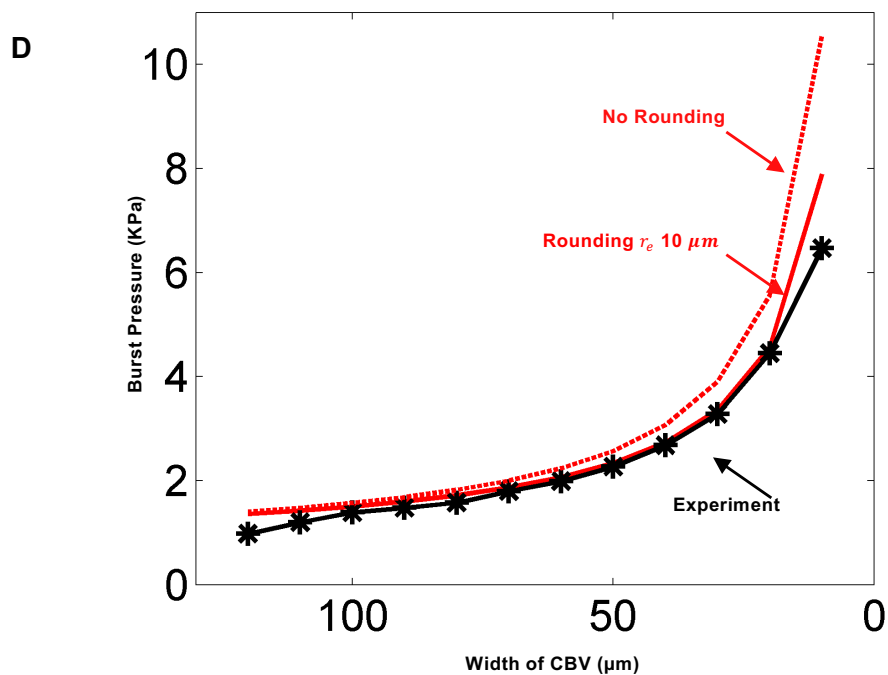
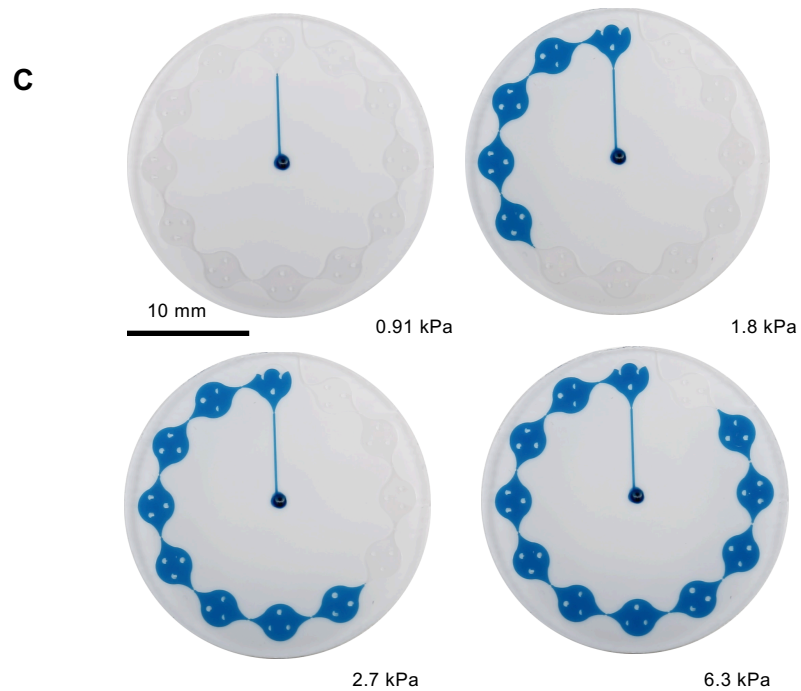
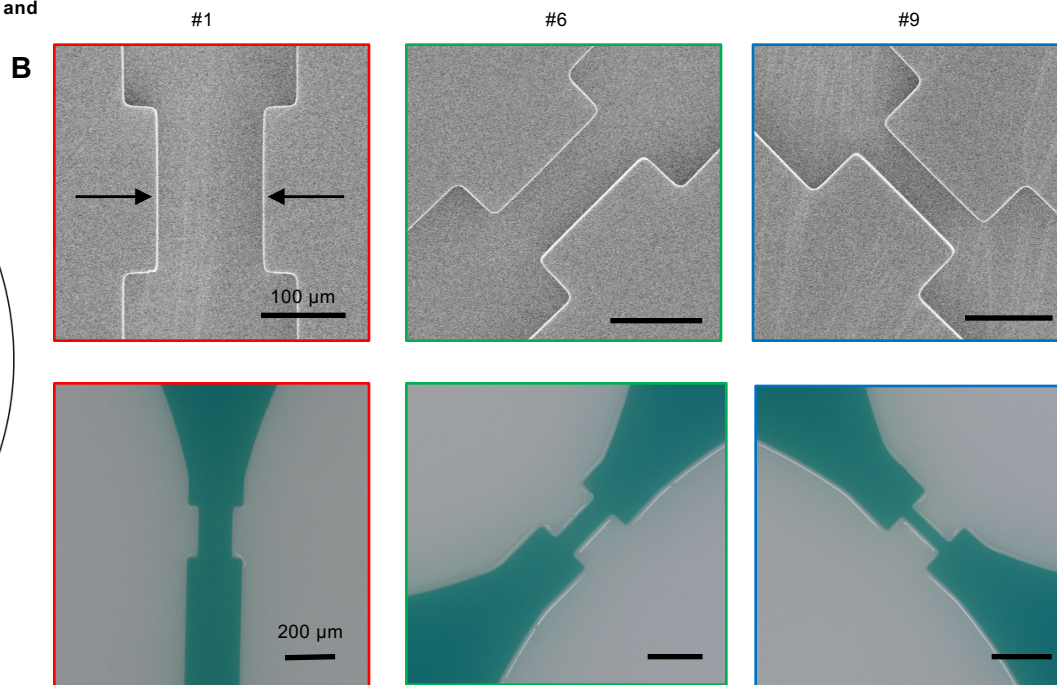
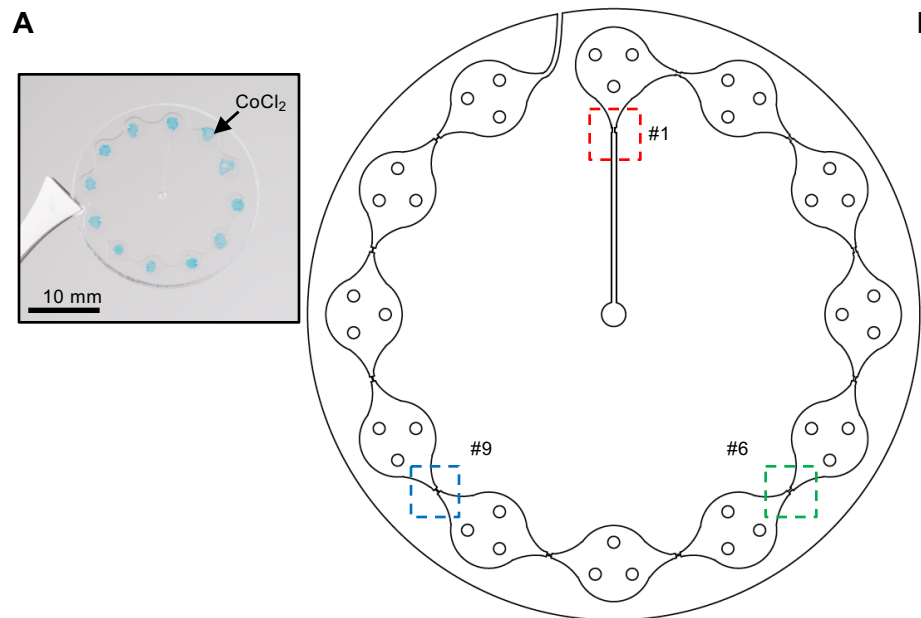


Fig. S10 SPSGs from various of region of the body with difference opening area to the skin at a) exercising condition at elliptical machine and b) a session at sauna. The left column is from the device of single CBVs and the right column is from the device of serial CBVs.

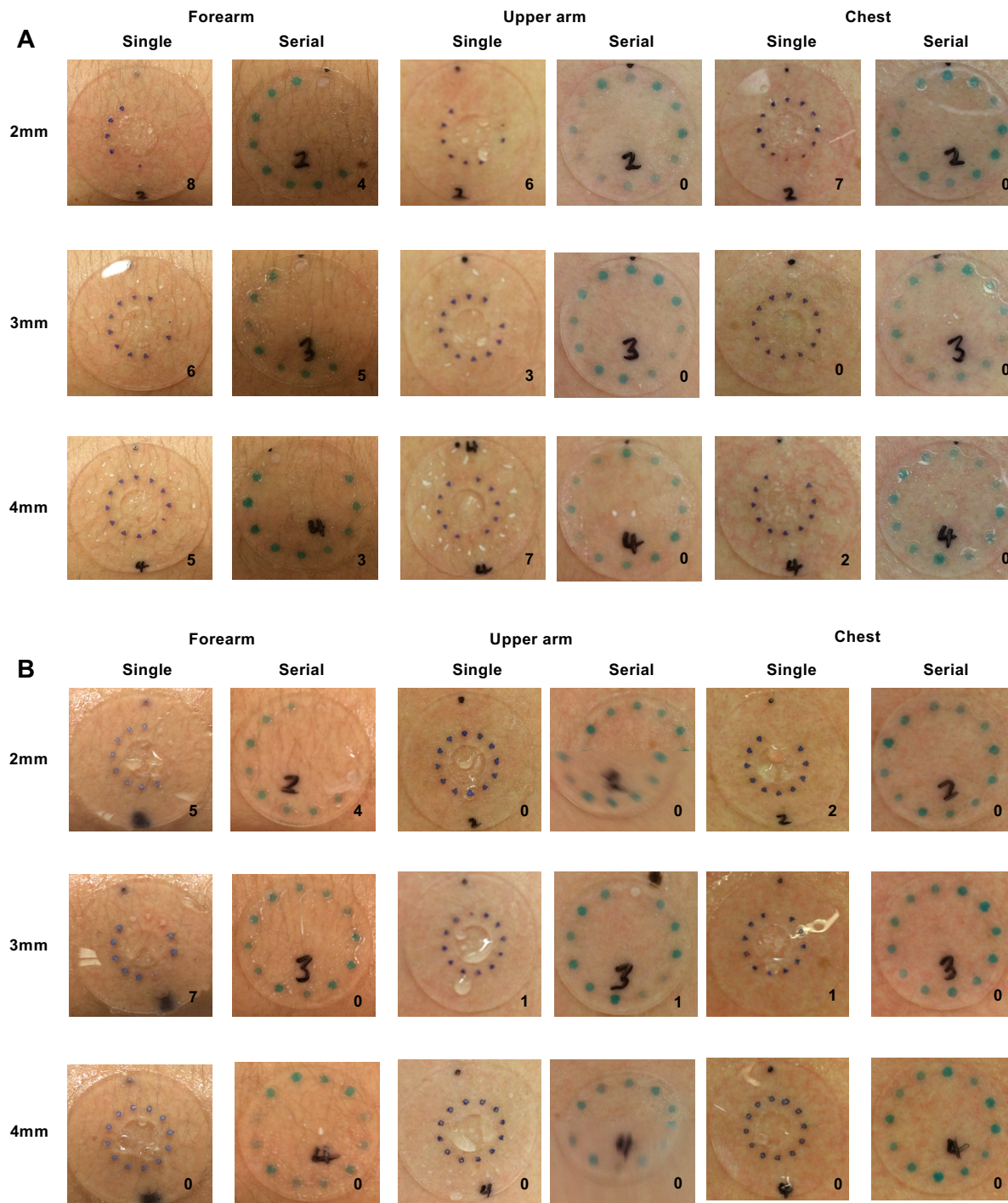


Fig. S11 Effect of the adhesive area to the sectary pressure of sweat glands. a) The SPSG of three regions of the body; forearm, upper arm and chest; with different adhesive area from 30 mm to 50 mm in diameter after 20 min of cycling. b) the graph of the summary of the effect of adhesive area to the SPSG. Scale bars represent 10mm.

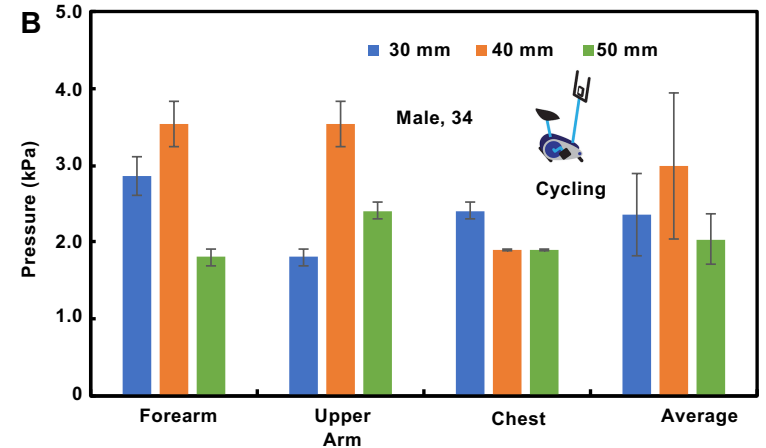
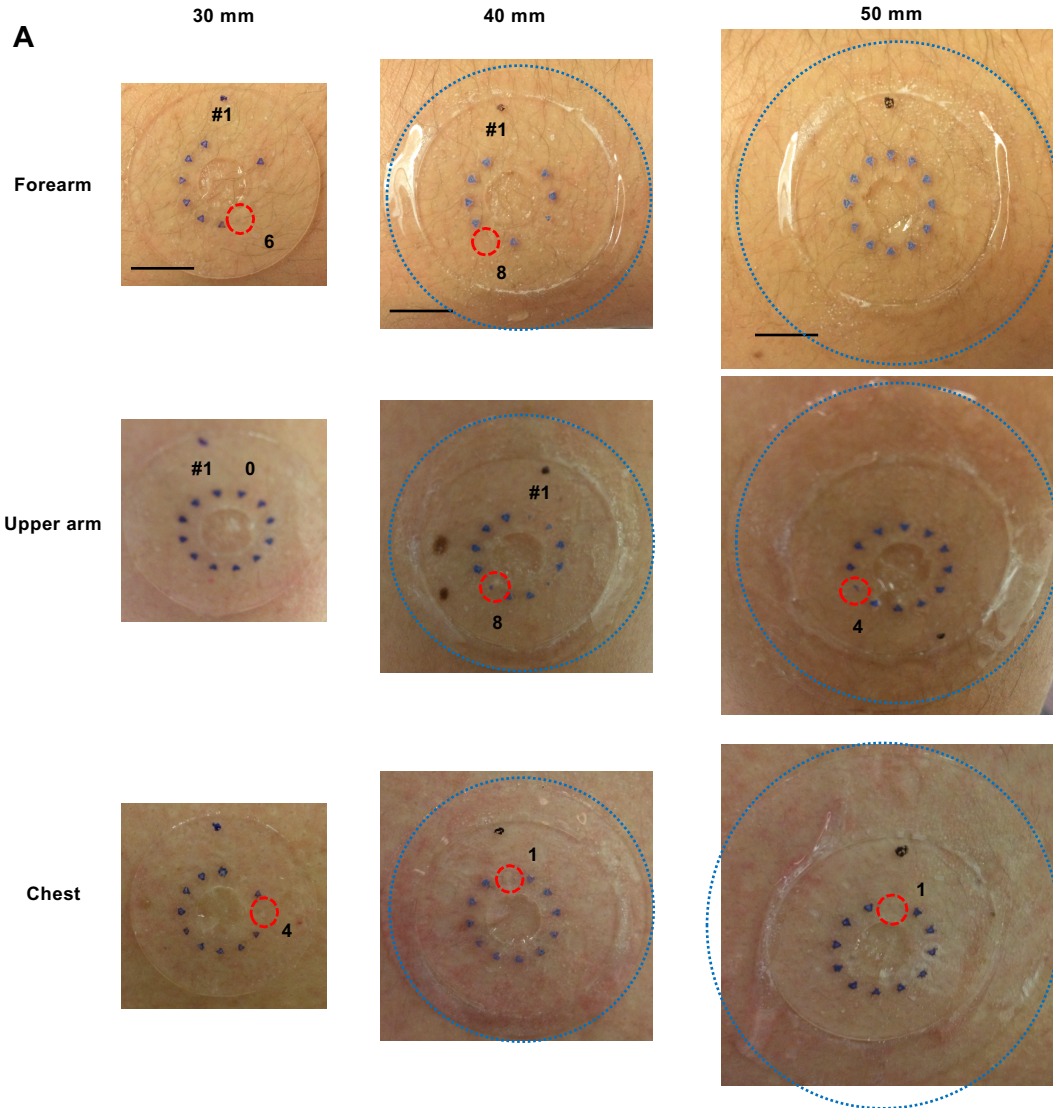


Fig. S12 Effect of the sweat rate to the sectary pressure of sweat glands. The SPSPG of forearm to different sweat rate during 30 min of cycling.

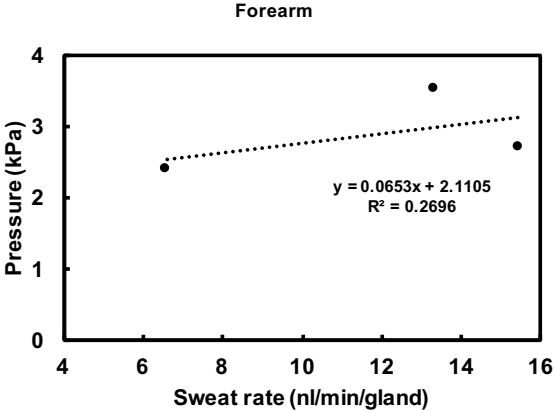


Fig. S13 SPSGs from various of region of the body including forehead and behind the ear at exercising condition at elliptical machine.

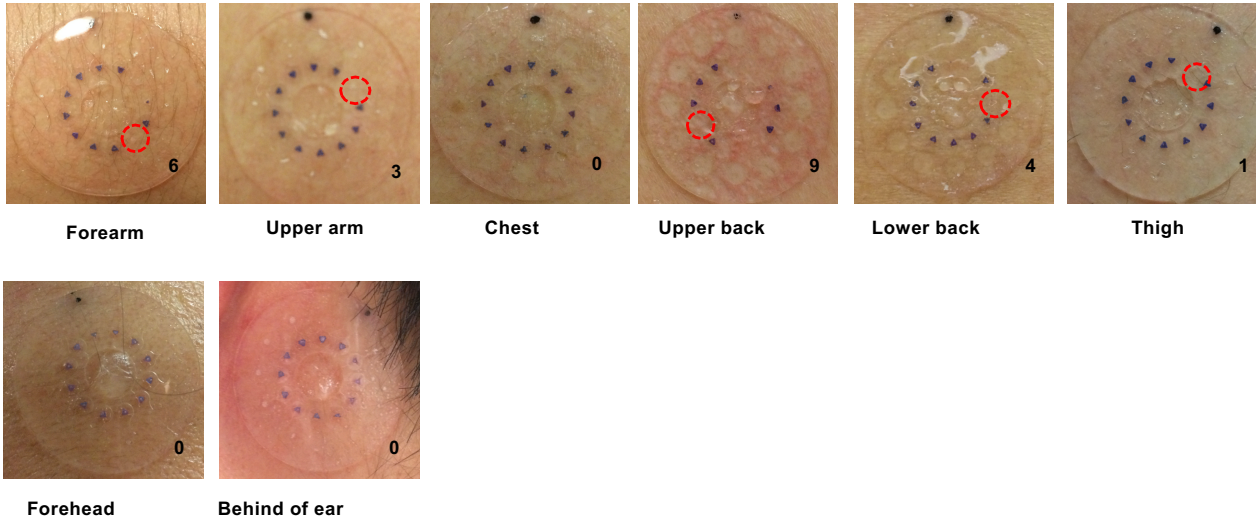
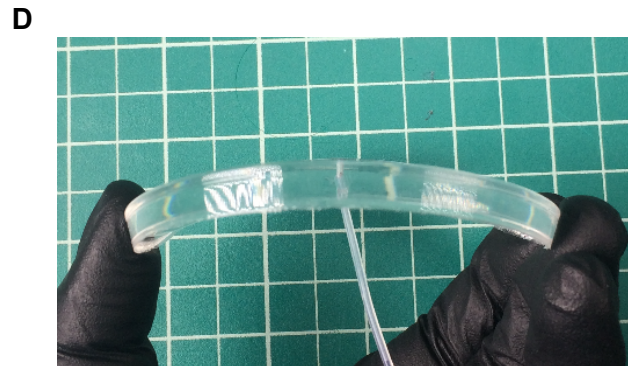
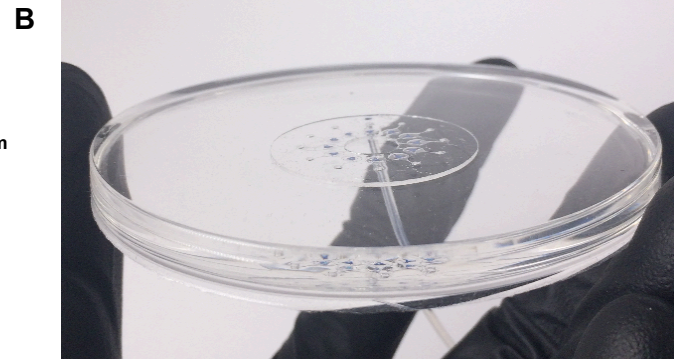
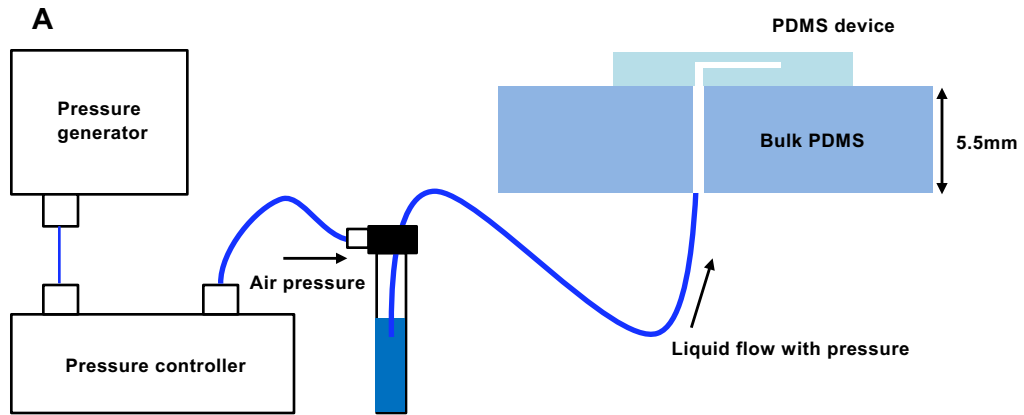


Fig. S14 Effect of the mechanical stresses to the bursting of CBVs. a) experimental set up to test the effect of the mechanical forces to the bursting of CBVs. b) optical image of pressure measuring device on the Bulk PDMS connected to the microfluidic controller. Optical images of device under mechanical stress c) compress d) stretch e) table of applied pressure on the valve according to the width of the valve during the mechanical stresses.



E

Width of CBV (μm)	Applying Pressure (kPa)
120	1.26
110	1.33
100	1.42
90	1.45
80	1.69
70	1.89
60	2.01
50	2.22
40	2.47
30	3.03
20	3.92
10	6.30

Table S1 The measured and calculated characteristics of the CBVs.

Nominal Width (μm)	Measured Width (μm)	Measured Rounding Radius (μm)	Measured Burst Pressure (In vitro test, kPa)	Uncertainty of bursting pressure (In vitro test, kPa)	Calculated Burst Pressure (with Rounding Correction, kPa)	Calculated Burst Pressure (without Rounding Correction, kPa)
10	11.41	12.93	9.00	0.62	10.05	13.51
20	18.67	11.26	5.60	0.50	6.96	8.62
30	27.43	14.10	4.33	0.25	5.11	6.16
40	41.16	11.82	3.53	0.29	3.91	4.42
50	54.94	10.47	3.17	0.31	3.25	3.54
60	64.85	12.39	2.87	0.25	2.89	3.14
70	69.31	12.24	2.70	0.10	2.78	3.00
80	82.14	10.81	2.41	0.10	2.53	2.67
90	94.04	11.77	2.07	0.21	2.33	2.45
100	105.77	11.80	2.03	0.21	2.18	2.28
110	114.57	9.18	1.90	0.01	2.11	2.18
120	130.86	10.11	1.80	0.11	1.96	2.02